

# Continuous Monitoring of Rabi Oscillations in a Josephson Flux Qubit

E. Il'ichev,<sup>1</sup> N. Oukhanski,<sup>1</sup> A. Izmailkov,<sup>1,2</sup> Th. Wagner,<sup>1</sup> M. Grajcar,<sup>3,4</sup> H.-G. Meyer,<sup>1</sup>  
A.Yu. Smirnov,<sup>5</sup> Alec Maassen van den Brink,<sup>5</sup> M.H.S. Amin,<sup>5</sup> and A.M. Zagorskin<sup>5,6,\*</sup>

<sup>1</sup>*Institute for Physical High Technology, P.O. Box 100239, D-07702 Jena, Germany*

<sup>2</sup>*Moscow Engineering Physics Institute (State University), Kashirskoe sh. 31, 115409 Moscow, Russia*

<sup>3</sup>*Department of Solid State Physics, Comenius University, SK-84248 Bratislava, Slovakia*

<sup>4</sup>*Friedrich Schiller University, Institute of Solid State Physics, D-07743 Jena, Germany*

<sup>5</sup>*D-Wave Systems Inc., 320-1985 W. Broadway, Vancouver, B.C., V6J 4Y3, Canada*

<sup>6</sup>*Physics and Astronomy Dept., The University of British Columbia,  
6224 Agricultural Rd., Vancouver, B.C., V6T 1Z1, Canada*

(Dated: September 12, 2018)

Under resonant irradiation, a quantum system can undergo coherent (Rabi) oscillations in time. We report evidence for such oscillations in a *continuously* observed three-Josephson-junction flux qubit, coupled to a high-quality tank circuit tuned to the Rabi frequency. In addition to simplicity, this method of *Rabi spectroscopy* enabled a long coherence time of about  $2.5\mu\text{s}$ , corresponding to an effective qubit quality factor  $\sim 7000$ .

PACS numbers: 03.67.Lx, 85.25.Cp, 85.25.Dq

Small superconducting devices can exist in superpositions of macroscopically distinct states, making them potential qubits [1]. In *flux qubits* such states are distinguished by a magnetic flux, corresponding to a circulating current  $\lesssim 1\mu\text{A}$ . Microwaves in resonance with the spacing between a qubit's energy levels will cause their occupation probabilities to oscillate, with a frequency proportional to the microwave amplitude. Such *Rabi oscillations* have been detected, using statistical analysis of the response to external pulses [2–5]. This requires precise pulse timing and shape, motivating our search for a complementary, continuous observation method.

The oscillations will only last for a coherence time from the instant the high-frequency (HF) signal is applied, after which the levels will be occupied almost equally. The system's *correlations*, however, will be affected by Rabi oscillation as long as the HF signal is on. Therefore, the signature of Rabi oscillations can be found in the auto-correlation function or its Fourier transform, the spectral density. In particular, if the qubit is coupled to a tank circuit, the spectral density of the tank-voltage fluctuations rises above the background noise when the qubit's Rabi frequency  $\omega_R$  coincides with the tank's resonant frequency  $\omega_T$ . This forms the basis for our measurement procedure of *Rabi spectroscopy*.

The qubit is described by the Hamiltonian

$$H = -\frac{1}{2}(\Delta\sigma_x + \epsilon\sigma_z) - W(t)\sigma_z, \quad (1)$$

with  $\Delta$  the tunnel splitting,  $\epsilon$  the DC energy bias, and  $W(t) = W \cos \omega_{\text{HF}} t$  the HF signal. For  $W = 0$ , the qubit levels  $|0\rangle$  and  $|1\rangle$  have energies  $\mp \frac{1}{2}\Omega$  respectively, where  $\Omega = \sqrt{\Delta^2 + \epsilon^2}$ . Rabi oscillations between these levels are induced near resonance  $\omega_{\text{HF}} \approx \Omega/\hbar$ . At resonance,

$$\hbar\omega_R = (\Delta/\Omega) W, \quad (2)$$

proportional to  $W$  ( $\propto \sqrt{P}$ , with  $P$  the HF power) [6].

Changes in qubit magnetic moment due to Rabi oscillation excite the tank. If photons in the latter have a sufficiently long lifetime, one can accumulate (hence the name “tank”) a sufficient number for their detection to be almost classical, while (for a small coupling coefficient) their emission from the qubit is still weak enough to disrupt the Rabi oscillation only occasionally. In detail, the qubit contribution to the nonequilibrium spectral density of the tank voltage is [7]

$$S_V(\omega, \omega_R) = 2 \frac{\epsilon^2}{\Omega^2} k^2 \frac{L_q I_q^2}{C_T} \omega_T^2 \Gamma(\omega) \frac{\omega_R^2}{(\omega^2 - \omega_R^2)^2 + \omega^2 \Gamma^2(\omega)} \times \frac{\omega_T^2}{(\omega^2 - \omega_T^2)^2 + \omega^2 \gamma_T^2}, \quad (3)$$

where  $\gamma_T$  ( $C_T$ ) is the damping rate (capacitance) of the tank circuit, and  $L_q$  ( $I_q$ ) is the inductance (persistent current) of the qubit loop. The tank-qubit coupling is  $k \equiv M/\sqrt{L_T L_q}$ , with  $M$  ( $L_T$ ) the mutual (tank) inductance. The effect vanishes at the degeneracy point  $\epsilon = 0$ , since both qubit eigenstates then have zero average persistent current [8]. Note that  $S_V$  in Eq. (3) has two factors: the first describes the qubit signal, the second its filtering by the tank's response function. Besides, the total tank spectrum  $S_{V,t}(\omega, \omega_R)$  has a background part  $S_b(\omega)$ , due to thermal and quantum damped-oscillator noise uncorrelated with the qubit contribution.

The qubit's total decoherence rate,

$$\Gamma(\omega) = \Gamma_0 + 4k^2 \frac{L_q I_q^2}{\hbar^2} \frac{\epsilon^2}{\Omega^2} \omega_T^2 \frac{\gamma_T k_B T}{(\omega^2 - \omega_R^2)^2 + \gamma_T^2 \omega_R^2}, \quad (4)$$

incorporates an internal contribution  $\Gamma_0$ , as well as a resonant one of the tank; see further Ref. [7]. If  $\Gamma = \Gamma(\omega_T) \gg \gamma_T$ , the peak value in  $\omega$  of  $S_V$  is reached at  $\omega_T$ :  $S_{V,\text{max}}(\omega_R) \propto \omega_R^2 / [(\omega_T^2 - \omega_R^2)^2 + \omega_T^2 \Gamma^2]$ . Thus,  $S_{V,\text{max}}(\omega_R)$  lies on a Lorentzian-type curve with a width determined

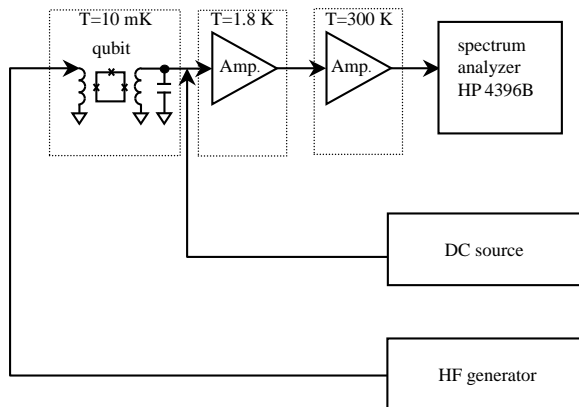


FIG. 1: Measurement setup. The flux qubit is inductively coupled to a tank circuit. The DC source applies a constant flux  $\Phi_e \approx \frac{1}{2}\Phi_0$ . The HF generator drives the qubit through a separate coil at a frequency close to the level separation  $\Delta/h = 868\text{MHz}$ . The output voltage at the resonant frequency of the tank is measured as a function of HF power.

by  $\Gamma$ . Hence, observing such a distribution not only is evidence for Rabi oscillations in the qubit, but also gives information about its coherence time.

We use a small-inductance superconducting loop interrupted by three Josephson junctions (a 3JJ qubit) [9], inductively coupled to a high-quality superconducting tank circuit [10] (Fig. 1). This approach is similar to the one in entanglement experiments with Rydberg atoms and microwave photons in a cavity [11]. The tank serves as a sensitive detector of Rabi transitions in the qubit, and simultaneously as a filter protecting it from noise in the external circuit. Since  $\omega_T \ll \Omega/\hbar$ , the qubit is effectively decoupled from the tank unless it oscillates with frequency  $\omega_T$ . That is, while *wide-band* (i.e., fast on the qubit time scale) detectors up to now have received most theoretical attention (e.g., [12]), we use *narrow-band* detection to have sufficient sensitivity at a single frequency even with a small coupling coefficient; cf. above Eq. (3). The tank voltage is amplified and sent to a spectrum analyzer. This is a development of the Silver–Zimmerman setup in the first RF-SQUID magnetometers [13], and is effective for probing flux qubits [14, 15]. As such, it was used to determine the potential profile of a 3JJ qubit in the classical regime [16].

The qubit was fabricated out of Al inside the tank’s pickup coil (Fig. 2). We aimed for the parameters suggested in Ref. [9]. Two junctions have areas  $200 \times 600\text{nm}^2$  and one is smaller, so that the critical currents have ratio  $\alpha \equiv I_{c3}/I_{c1,2} \approx 0.8$ . The tank was fabricated using a Nb thin-film pancake coil on an oxidized Si substrate. It has  $\omega_T/2\pi = 6.284\text{MHz}$ , consistent with the estimated  $L_T = 0.2\mu\text{H}$  and  $C_T = 3\text{nF}$ . The qubit has  $L_q = 24\text{pH}$ ; the larger junctions have  $C_q = 3.9\text{fF}$  and  $I_{c1,2} = 600\text{nA}$ . The tank’s quality factor  $Q_T \equiv \omega_T/2\gamma_T = 1850$  corresponds to a linewidth  $\sim 1.7\text{kHz}$ , while  $M = 70\text{pH}$ . The

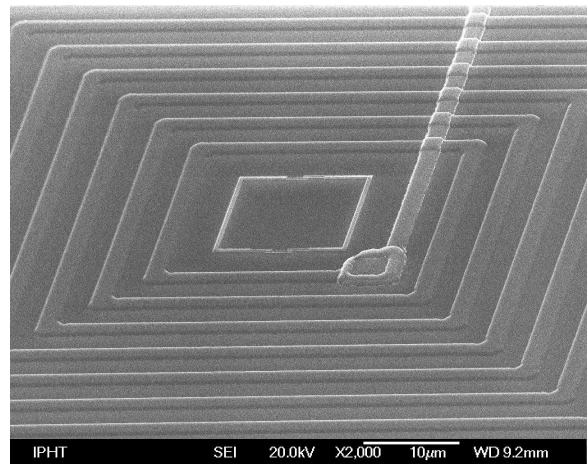


FIG. 2: The Al qubit inside the Nb pancake coil.

noise temperature of the cold amplifier is  $\sim 300\text{mK}$  [17].

The qubit loop encloses an external magnetic flux  $\Phi_e$ . Its total Josephson energy is  $E_J = \sum_{i=1}^3 E_{Ji}(\phi_i)$ , where  $\phi_i$  and  $E_{Ji} = \hbar I_{ci}/2e$  are the phase difference and Josephson energy of the  $i$ th junction. Due to flux quantization and negligible  $L_q$ , only  $\phi_{1,2}$  are independent, with  $\phi_3 = -\phi_1 - \phi_2 - 2\pi\Phi_e/\Phi_0$  ( $\Phi_0 = h/2e$  is the flux quantum). The quantum dynamics in the resulting potential  $E_J(\phi_1, \phi_2)$  is determined by the ratio of  $E_J$  and the Coulomb energy  $E_C \sim e^2/C_q \ll E_J$ . For suitable parameters, at  $\Phi_e = \frac{1}{2}\Phi_0$  the system has degenerate classical minima  $|L\rangle$  and  $|R\rangle$ , with persistent currents circulating in opposite directions [9]. A finite  $E_C$  lifts the degeneracy by allowing tunneling between these minima, and opens a gap  $\Delta$  at the anticrossing between the ground and first excited states,  $|0, 1\rangle = (|L\rangle \pm |R\rangle)/\sqrt{2}$ . Hence, the qubit can be treated as a two-level system described by Eq. (1).

To measure  $S_V$ , we tuned the HF signal in resonance with the qubit [8]. We only found noticeable output when  $\omega_{\text{HF}}/2\pi = 868 \pm 2\text{MHz}$ , in agreement with the estimated splitting  $\Delta/h \sim 1\text{GHz}$ . One important feature of our setup is a two orders of magnitude mismatch between  $\omega_{\text{HF}}$  and the readout frequency  $\omega_T$ . Together with the high  $Q_T$ , this ensures that the signal can only be due to resonant transitions in the qubit itself. This was verified by measuring  $S_V$  also when biasing the qubit away from degeneracy. A signal exceeding the background, that is, emission of  $\sim 6\text{MHz}$  photons by the qubit in response to a resonant HF field in agreement with Eq. (3), was only detected when the qubit states were almost [cf. below Eq. (4)] degenerate. The measurements were carried out at  $T = 10\text{mK}$ . No effect of radiation was observed above  $40\text{mK}$  (with  $40\text{mK}/\hbar k_B \approx 830\text{MHz}$ , i.e. close to  $\Delta/h$ ).

We plotted  $S_{V,t}(\omega)$  for different HF powers  $P$  in Fig. 3. As  $P$  is increased,  $\omega_R$  grows and passes  $\omega_T$ , leading to a non-monotonic dependence of the maximum signal on  $P$  in agreement with the above picture. This, and the sharp

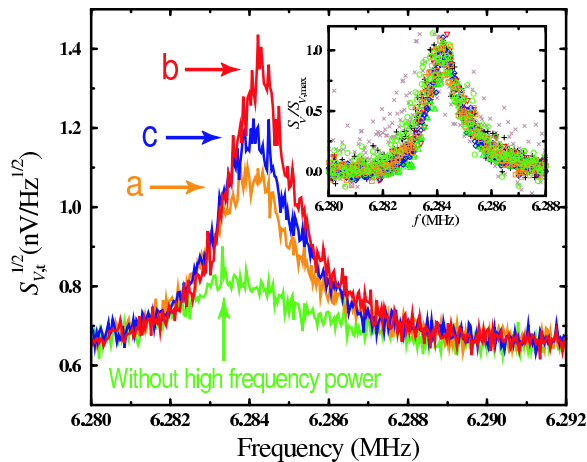


FIG. 3: The spectral amplitude of the tank voltage for HF powers  $P_a < P_b < P_c$  at 868MHz, detected using the setup of Fig. 1. The bottom curve corresponds to the background noise without an HF signal. The inset shows normalized voltage spectra for seven values of HF power, with background subtracted. The shape of the resonance, being determined by the tank circuit, is essentially the same in each case. Remaining tiny variations visible in the main figure are due to the irradiated qubit modifying the tank's inductance and hence its central frequency, and in principle similarly for dissipation in the qubit increasing the tank's linewidth [7]; these are inconsequential for our analysis.

dependence on the tuning of  $\omega_{\text{HF}}$  to the qubit frequency, confirm that the effect is due to Rabi oscillations. The inset shows that the shape is given by the second line of Eq. (3) for all curves.

For a quantitative comparison between theory and experiment, we subtracted the background without an HF signal from the observed  $S_{V,t}$ , yielding  $S_V(\omega) = S_{V,t}(\omega) - S_b(\omega)$  [18]. Subsequently, we extracted the peak values vs HF amplitude,  $S_{V,\text{max}}(\sqrt{P/P_0}) = \max_{\omega} S_V(\omega) \approx S_V(\omega_T)$ , where  $P_0$  is the power causing the maximum response; see Fig. 4a. In the same figure, we plot the theoretical curve for  $S_{V,\text{max}}$  normalized to its maximum  $S_0$ ,

$$\frac{S_{V,\text{max}}(w)}{S_0} = \frac{w^2 g^2}{(w^2 - 1)^2 + g^2} \approx \frac{(g/2)^2}{(w-1)^2 + (g/2)^2}; \quad (5)$$

$w \equiv \omega_R/\omega_T$  ( $= \sqrt{P/P_0}$  theoretically) and  $g = \Gamma/\omega_T$ . The best fit is found for  $\Gamma \approx 0.02\omega_T \sim 8 \cdot 10^5 \text{s}^{-1}$  [19]. Thus, the life-time of the Rabi oscillations is at least  $\tau_{\text{Rabi}} = 2/\Gamma \approx 2.5 \mu\text{s}$  [20], leading to an effective quality factor  $Q_{\text{Rabi}} = \Delta/(\hbar\Gamma) \sim 7000$ . These values substantially exceed those obtained recently for a modified 3JJ qubit ( $\tau_{\text{Rabi}} \sim 150\text{ns}$ ) [5], which is not surprising. In our setup the qubit is read out not with a dissipative DC-SQUID, but with a high-quality resonant tank. The latter is weakly coupled to the qubit ( $k^2 \sim 10^{-3}$ ), suppressing the noise leakage to it.

Finally, we can restore  $\omega_R(\sqrt{P})$ . Assuming the spectrum to be described by Eq. (5) with  $\Gamma = 0.02\omega_T$ , we

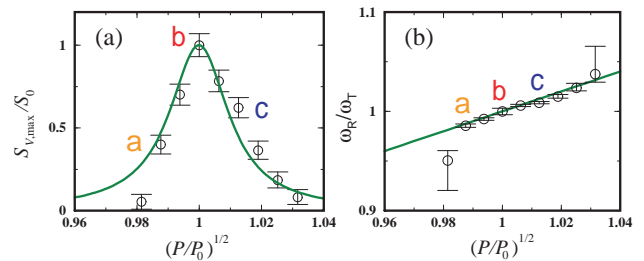


FIG. 4: (a) Comparing the data to the theoretical Lorentzian. The fitting parameter is  $g \approx 0.02$ . Letters in the picture correspond to those in Fig. 3. (b) The Rabi frequency extracted from (a) vs the applied HF amplitude. The straight line is the predicted dependence  $\omega_R/\omega_T = \sqrt{P/P_0}$ . The good agreement provides strong evidence for Rabi oscillations.

correlate the experimental and theoretical points giving the same normalized value:  $[S_{V,\text{max}}(\omega_R/\omega_T)/S_0]_{\text{theor}} = [S_{V,\text{max}}(\sqrt{P/P_0})/S_0]_{\text{exp}}$ . Figure 4b confirms the linear dependence  $\omega_R/\omega_T = \sqrt{P/P_0}$  [Eq. (2)], given by the line.

In conclusion, we have observed Rabi oscillations in a three-junction flux qubit coupled to a resonant tank circuit. The oscillation frequency depends linearly on the applied HF amplitude, as predicted. The method of Rabi spectroscopy does not require precise pulse timing. A lower bound on the coherence time is  $2.5 \mu\text{s}$ . The qubit's coherence survives its coupling to the external tank circuit, to the extent that  $\tau_{\text{Rabi}}$  is  $\sim 16$  times the Rabi period. All main features have been reproduced in a second sample with  $\omega_{\text{HF}}/2\pi = 3.665\text{GHz}$  and  $\omega_T/2\pi = 27.5\text{MHz}$  (data not shown), though with a somewhat lower  $Q_{\text{Rabi}}$ . Thus, high-quality superconducting tanks provide a straightforward and sensitive method for qubit characterization; their use as coupling elements between qubits is actively being researched [21].

We thank D. Born and H. Mühlig for technical assistance; U. Hübner, T. May, and I. Zhilyaev for sample fabrication; and I. Chiorescu, Ya.S. Greenberg, W. Hardy, J.P. Hilton, H.E. Hoening, Y. Imry, W. Krech, Y. Nakamura, G. Rose, A. Shnirman, P.C.E. Stamp, M.F.H. Steininger, and W.G. Unruh for fruitful discussions.

\* Electronic address: [zagoskin@dwavesys.com](mailto:zagoskin@dwavesys.com)

- [1] Y. Makhlin, G. Schön, and A. Shnirman, Rev. Mod. Phys. **73**, 357 (2001).
- [2] Y. Nakamura, Yu.A. Pashkin, and J.S. Tsai, Phys. Rev. Lett. **87**, 246601 (2001).
- [3] D. Vion, A. Aassime, A. Cottet, P. Joyez, H. Pothier, C. Urbina, D. Esteve, and M.H. Devoret, Science **296**, 886 (2002).
- [4] J.M. Martinis, S. Nam, J. Aumentado, and C. Urbina, Phys. Rev. Lett. **89**, 117901 (2002).
- [5] I. Chiorescu, Y. Nakamura, C.J.P.M. Harmans, and J.E. Mooij, Science **299**, 1869 (2003).

- [6] As in Refs. [2–5],  $\omega_R$  here is the angular frequency of *probability* oscillations. After one resonant oscillation, the *wave function* has changed its sign. In cases where this is relevant, defining the Rabi frequency twice as small is advantageous—e.g., M.H.S. Amin, A.Yu. Smirnov, and A. Maassen van den Brink, Phys. Rev. B **67**, 100508(R) (2003).
- [7] A.Yu. Smirnov, cond-mat/0306004.
- [8] C.H. van der Wal, A.C.J. ter Haar, F.K. Wilhelm, R.N. Schouten, C.J.P.M. Harmans, T.P. Orlando, S. Lloyd, and J.E. Mooij, Science **290**, 773 (2000).
- [9] J.E. Mooij, T.P. Orlando, L. Levitov, L. Tian, C.H. van der Wal, and S. Lloyd, Science **285**, 1036 (1999).
- [10] E. Il'ichev *et al.*, Rev. Sci. Instr. **72**, 1882 (2001).
- [11] J.M. Raimond, M. Brune, and S. Haroche, Rev. Mod. Phys. **73**, 565 (2001).
- [12] A.N. Korotkov and D.V. Averin, Phys. Rev. B **64**, 165310 (2001).
- [13] A.H. Silver and J.E. Zimmerman, Phys. Rev. **157**, 317 (1967).
- [14] Ya.S. Greenberg, A. Izmalkov, M. Grajcar, E. Il'ichev, W. Krech, H.-G. Meyer, M.H.S. Amin, and A. Maassen van den Brink, Phys. Rev. B **66**, 214525 (2002).
- [15] Ya.S. Greenberg, A. Izmalkov, M. Grajcar, E. Il'ichev, W. Krech, and H.-G. Meyer, Phys. Rev. B **66**, 224511 (2002).
- [16] E. Il'ichev *et al.*, Appl. Phys. Lett. **80**, 4184 (2002).
- [17] N. Oukhanski, M. Grajcar, E. Il'ichev, and H.-G. Meyer, Rev. Sci. Instr. **74**, 1145 (2003).
- [18] Without an HF signal, the qubit's influence at  $\omega_T$  is negligible. Thus, the “dark” trace in Fig. 3 is a quantitative measure of  $S_b$ .
- [19] Since the tank damping is  $\gamma_T \sim 3000\text{s}^{-1}$ , this justifies our approximation  $\Gamma \gg \gamma_T$ .
- [20] This may in fact exceed the intrinsic “free-induction” coherence time  $\tau_\phi$ , as already evidenced by the factor 2 in  $\tau_{\text{Rabi}}$ . Cf. the concluding remarks in [5].
- [21] F. Plastina and G. Falci, Phys. Rev. B **67**, 224514 (2003); A. Blais, A. Maassen van den Brink, and A.M. Zagoskin, Phys. Rev. Lett. **90**, 127901 (2003); A.Yu. Smirnov and A.M. Zagoskin, cond-mat/0207214.